

Supporting Information for
Folding Artificial Mucosa with Cell-Laden Hydrogels Guided by Mechanics Models

Hon Fai Chan^{a,b,c,d,1}, Ruike Zhao^{a,e,1}, German A. Parada^{a,f}, Hu Meng^{c,d}, Kam W. Leong^g, Linda G. Griffith^{a,b}, Xuanhe Zhao^{a,h,2}

^a Department of Mechanical Engineering, Massachusetts Institute of Technology, Cambridge, MA, 02139

^b Department of Biological Engineering, Massachusetts Institute of Technology, Cambridge, MA, 02139

^c Institute for Tissue Engineering and Regenerative Medicine, The Chinese University of Hong Kong, Hong Kong, China

^d School of Biomedical Sciences, The Chinese University of Hong Kong, Hong Kong, China

^e Department of Mechanical and Aerospace Engineering, The Ohio State University, Columbus, OH, 43210, USA

^f Department of Chemical Engineering, Massachusetts Institute of Technology, Cambridge, MA, 02139

^g Department of Biomedical Engineering, Columbia University, New York, NY, 10027

^h Department of Civil and Environmental Engineering, Massachusetts Institute of Technology, Cambridge, MA 02139

¹ H.F.C and R.Z. contributed equally to this work.

² Correspondence should be addressed to Prof. Xuanhe Zhao. Email: zhaox@mit.edu. Address: 77 Massachusetts Ave, 1-310D, Cambridge, MA, 02139. Phone: 617.253.5328

Keywords: mucosa | hydrogel | mechanical instability | tissue engineering | biomechanics

This file includes

- 1. Supplementary Methods**
- 2. Supplementary figures and figure captions 1 to 8**
- 3. Supplementary Table 1**

Supplementary Methods

Finite-element method for predicting the morphologies of the film-substrate system

The 2D and 3D finite-element models are established to calculate the surface instabilities that developed on the surface of the uniaxially and biaxially loaded GelMA-tough hydrogel (film-substrate) structure, respectively. The simulations are implemented by commercial software package Abaqus (2016) with plane-strain element CPE4RH and 3D stress element C3D8RH for the uniaxial and biaxial cases, respectively. Both film and substrate are represented by incompressible neo-Hookean material which has the strain energy density of

$$U = \frac{\mu}{2} \left[(\lambda_1^2 + \lambda_2^2 + \lambda_3^2) - 3 \right] - p(J - 1) , \quad (S1)$$

where μ is the shear modulus of the material which is measured from experiment, p is the hydrostatic pressure which is determined by boundary conditions, and λ_i are the principal stretches, $J = \lambda_1 \lambda_2 \lambda_3$. While PAAm-alginate hydrogel is viscoelastic, we used the relaxed shear modulus to predict the surface patterns formed on it.

In the simulation implementation, prior to the substrate stretching, a very small amplitude sinusoidal imperfection with analytically calculated wavelength is applied to the film surface to probe any instability in the system. A self-contact interaction (frictionless and “hard contact”) is applied to the film surface to avoid penetration during creasing and folding deformations.

Additional Materials Used

Type A gelatin (300 bloom, porcine skin) (G2500; Sigma-Aldrich) and methacrylic anhydride (276685; Sigma-Aldrich) were used for GelMA synthesis. PARAFILM® M (Parafilm; P7793; Sigma-Aldrich) was used as spacer to make hydrogel film. Sylgard 184 [polydimethylsiloxane (PDMS; Dow Corning) was molded and activated with benzophenone (B9300; Sigma-Aldrich) for bonding with hydrogel. 1/8" acrylic sheets (8536K134, McMaster-Carr) were used for stretching the hydrogel substrate. FEP Optically Clear Tape (23-FEP-2-5, CS Hyde) was used to prevent GelMA adhesion to cover glass during photocrosslinking. Rhodamine b (R6626; Sigma-Aldrich) was used for confocal imaging the surface feature. Live/Dead cell imaging kit (R37601; Life Technologies) was used for cell viability assay. Blue fluorescent microsphere (F-8837; Life Technologies) was used as visualization the bonding between the film and the substrate. Rhodamine phalloidin (50646256; Fisher Scientific) was used to stain both Ishikawa cells and tHESCs while CK 18 Monoclonal Antibody (LDK18) - Alexa Fluor 488 (53-9815-82; Life Technologies) was used to stain Ishikawa cells specifically. Hoechst 33342 (H3570; Life Technologies) was used to stain cell nuclei. Rat tail collagen (354236; Corning) and Sulfo-SANPAH (22589; Thermo Fisher) were used to functionalize the surface of tough-hydrogel substrate for cell culture. FM™ 1-43 Dye (T35356; Thermo Fisher) was used to detect cell membrane damage.

Fabrication of folded hydrogel system

To fabricate folded hydrogel, approximately 1 mm thick PAAm-alginate hydrogel sheet was prepared by pressing pregel solution [12 wt% AAm, 0.012 wt% MBAA, 2mM APS, 2 wt%

alginate, CaSO₄ (20×10^{-3} M concentration in gel) and TEMED (8.2 μ l for every 10mL pregel solution)] between two layers of glass separated by 6 layers of parafilm and cured for 60 min at 50°C. The hydrogel sheet was then soaked in 20 wt% AAm, 0.2% Irgacure 2959, 0.012% MBAA for overnight for robust bonding with PDMS. The surface of PDMS was treated with 10% (wt/vol) benzophenone solution in ethanol for 10 min, washed, and dried with nitrogen. Thereafter, hydrogel sheet was pressed against two PDMS holders on two sides with a spacing of 1.2 cm and exposed to UV irradiation (365 nm; UVP CL-1000) for 30 min for assembly. The resultant hydrogel with holders was soaked in DPBS for overnight to remove unreacted chemical residuals, resulting in an increase thickness to 1.5 mm. An acrylic block made with different lengths (1.8 cm, 2.4 cm, 3 cm) using an Epilog laser machine were inserted underneath the tough hydrogel with holders for stretching. GelMA pregel solution (5 or 10 wt% GelMA, 0.7% Irgacure 2959) was added on the surface and pressed against with glass taped with optically clear FEP separated with spacer. Single layer of parafilm were used as spacer. After UV irradiation (Beauties Factory 9W UV lamp) for 5 min, the glass was removed and the tough hydrogel was removed from the acrylic block so that it would return to its original length to create fold on GelMA.

For biaxial folding, the tough-hydrogel sheet was bonded to four PDMS holders on four sides with a spacing of 1.2 cm. After soaked in DPBS for overnight, the tough hydrogel with holders was stretched by inserting a square acrylic block (1.8 cm in length and width) underneath. GelMA of thickness of $\sim 100 \mu\text{m}$ was crosslinked on top of the hydrogel-PDMS. Finally, the acrylic block was removed to generate the biaxial fold pattern.

Cell Culture

Ishikawa human endometrial adenocarcinoma cells (Sigma-Aldrich) and hTERT-immortalized human endometrial stromal cells (tHESCs) (ATCC) were routinely cultured in a humidified atmosphere at 37⁰C and 5% CO₂ in phenol red-free DMEM/F12 (mixture of Dulbecco's Modified Eagle's Medium and Ham's F-12 (Gibco) media) supplemented with 1% penicillin/streptomycin (Gibco) and 10% v/v dextran/charcoal treated fetal bovine serum (Atlanta Biologicals). Epithelial cells were split 1 : 6 and stromal cells were split 1 : 3 once they reached 70–80% confluency, and medium was replaced every 3 days. The cell lines were used prior to passage 25.

Synthesis of GelMA

GelMA was synthesized as described (1). Briefly, type A gelatin was dissolved at 10% w/v in a PBS solution at 50°C under constant stirring. Methacrylic anhydride (MA) was added slowly until the desired target was reached, and the mixture was allowed to react for an hour (Final MA vol.% was 20%). The reaction was stopped by diluting the mixture in PBS (fivefold excess) and then dialyzed for a week against water to remove salts and unreacted MA. The product, GelMA, was freeze-dried and stored at -20C until further use.

Measurement of the shear moduli of the GelMA-tough hydrogel system

The shear moduli of the GelMA film and tough hydrogel base were measured using universal machine (2 kN load cell; Zwick/Roell Z2.5). Before testing, the tough-hydrogel was

soaked in DPBS for overnight. The samples were uniaxially stretched at low strain rate [$0.01 \times \text{original length (mm} \times \text{s}^{-1})$] and the resultant force-displacement information was obtained. We then calculated the stress-stretch relation and fit the curve with neo-Hookean material constitutive equation as shown in Supplementary Information **Fig. S2**.

Culture of stromal and epithelial cells in the folded system

tHESCs suspension (1.6×10^7 per ml in culture medium) was mixed with GelMA pregel solution (final concentration at 10 wt% GelMA and 0.7% Irgacure 2959) at 1:10 ratio and added on top of a stretched tough-hydrogel substrate. It was then pressed against with glass taped with FEP separated with spacer. After UV irradiation for 5 min, the glass was removed and tension was released to create folded hydrogel with stromal component.

To supplement epithelium into the system, the bilayer hydrogel with tHESCs encapsulated in stretched state was transferred to culture medium. Ishikawa cell suspension (0.5×10^6 cells per cm^2) was pipetted on top of the hydrogel and the hydrogel was let sit for 15 min for cells to settle on the surface. The co-culture system was cultured at 37°C and 5% CO_2 with culture medium replenished every 3 days until a confluent epithelium was formed. Afterwards, tension was released and folded hydrogel with both stromal and epithelial components were created.

Confocal microscopy

To visualize the patterned mucosa under confocal microscopy, a few drops of rhodamine b ($1\mu\text{M}$) was added onto the folded hydrogel so that it would diffuse into the GelMA layer in a few minutes. It was then imaged using Leica SP8 upright confocal microscope. Z-stack images at $\sim 17\mu\text{m}$ per slide thickness were imaged and a 3D reconstruction image was created using the LAX S 3D visualization software. ImageJ was used to quantify the dimensions of the features generated based on images collected from 3 independent experiments. To visualize bonding between the film and substrate, blue fluorescent microspheres in solution form was used to dissolve GelMA to prepare the pregel solution. They were also mixed with tough-hydrogel during the preparation of hydrogel at lower densities ($\sim 1:10$ dilution). The folded GelMA was formed and z-stack images were taken and 3D reconstruction images were created.

Cell Viability assay

The folded hydrogel with stromal or/and epithelium components was washed in PBS twice before incubated in the Live/Dead cell imaging solution prepared according to instructions for 15 min. The folded hydrogel was then imaged using Leica SP8 upright confocal microscope. Z-stack images at $\sim 5\mu\text{m}$ per slide thickness were taken and a 3D reconstruction image was created using the LAX S 3D visualization software. In the case of co-culture of stromal and epithelium components, since the fluorescent signal was attenuated in the hydrogel, the intensities of tHESCs and Ishikawa cells were different. Therefore, two sets of z-stack images were taken at different gains to visualize two components separately. ImageJ software was used to integrate the two components into one single 3D reconstruction image. To quantify cell

viability, ImageJ was used to count the number of live and dead cells from images obtained in 3 independent experiments. To quantify average cell compressive strain and orientation of encapsulated tHESCs, ImageJ was used to obtain the major axis, minor axis and angle of each cell by fitting an ellipse to it. >150 cells were analyzed from each of the 3 images obtained in 3 independent experiments.

Immunofluorescence staining

Samples were fixed in a 4% paraformaldehyde PHEM buffer (Electron Microscopy Sciences) for 10 min and permeabilized in 0.1% TritonX-100 in PBS (Sigma-Aldrich) for 10 min. The samples were then incubated with either CK-18 antibody conjugated with Alexa Fluor 488 and/or rhodamine phalloidin in dark for 1 hr according to instructions provided. Hoechst 33342 was added to label the cell nuclei. The samples were washed in PBS twice before imaged using the Leica SP8 upright confocal microscope. Z-stack images were acquired following procedures described above for visualizing the 3D structure.

Examination of cell response to stretching between folded and flat epithelia

Ishikawa cells (0.5×10^6 cells per cm^2) were seeded on folded GelMA ($\lambda_{ps} = 2$) attached to tough-hydrogel or on flat tough-hydrogel hydrogel substrate directly after the surface was covalently functionalized with rat collagen I using Sulfo-SANPAH (2). After a mostly confluent epithelium was formed, cells were stained with Hoechst 33342 and FMTM 1-43. FMTM 1-43 is membrane impermeable and becomes fluorescent when it enters injured cells and binds to the

endomembrane. Nuclei shape and dye entry into the cells was monitored before and after stretching of the substrate for 100% with Leica SP8 upright confocal microscope.

Statistical Analysis

Data were expressed as average \pm standard deviation of the mean (S.D.). Statistical analysis was performed using GraphPad Prism 5. One-way ANOVAs with Tukey post-tests were performed to determine any significant difference in cell viability of encapsulated tHESCs in different folded GelMAs.

Supplementary Figures, Figure Captions 1 to 7 and Table 1

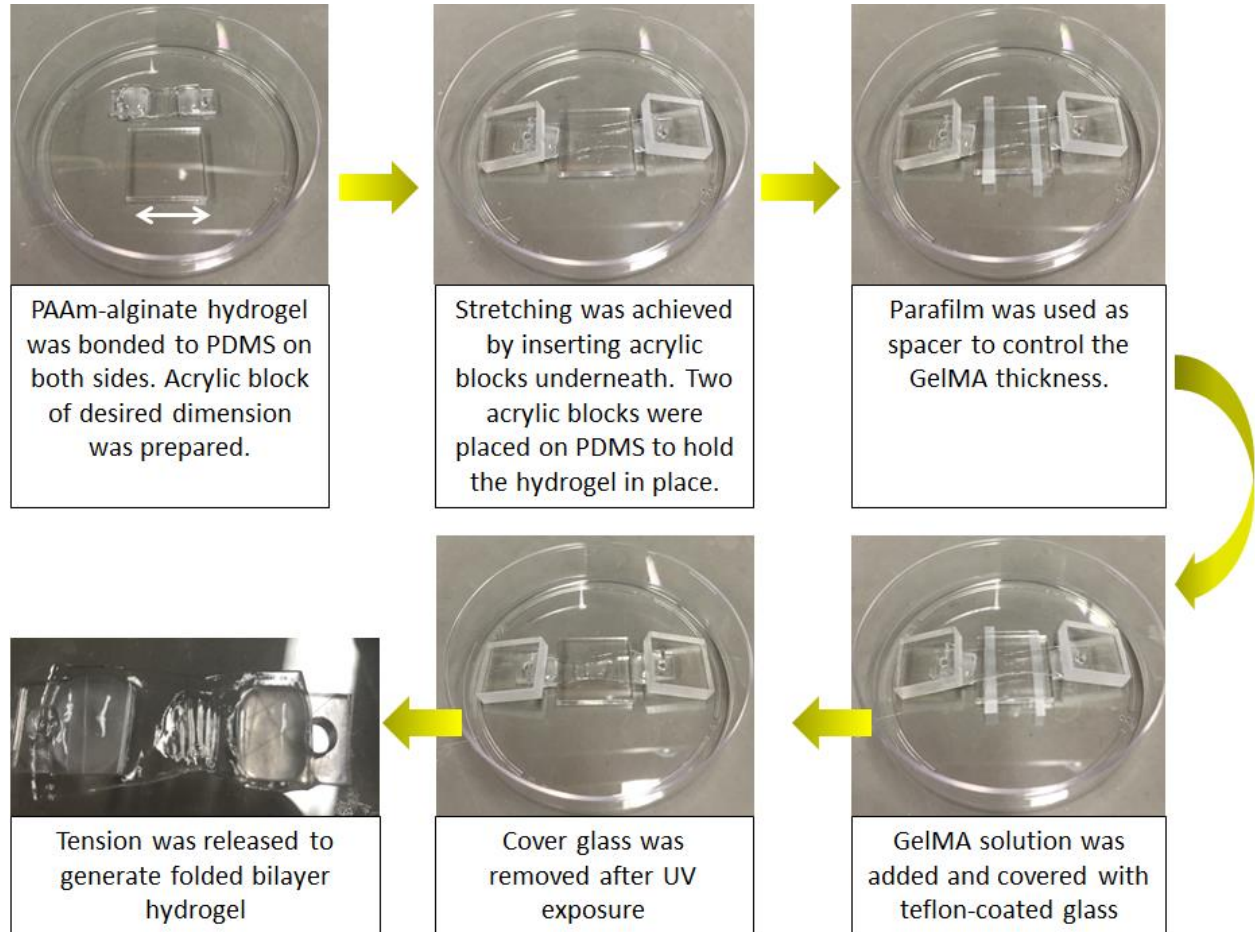


Figure S1. Procedures of fabricating uniaxial pattern. PAAm-alginate tough hydrogel is first bonded to two PDMS holders. Tough-hydrogel is then stretched uniaxially. Parafilm is used as spacer to control film thickness. After a cell-laden GelMA film is crosslinked via UV irradiation on the pre-stretched tough-hydrogel, tension is released to apply compressive strain to generate desired uniaxial pattern.

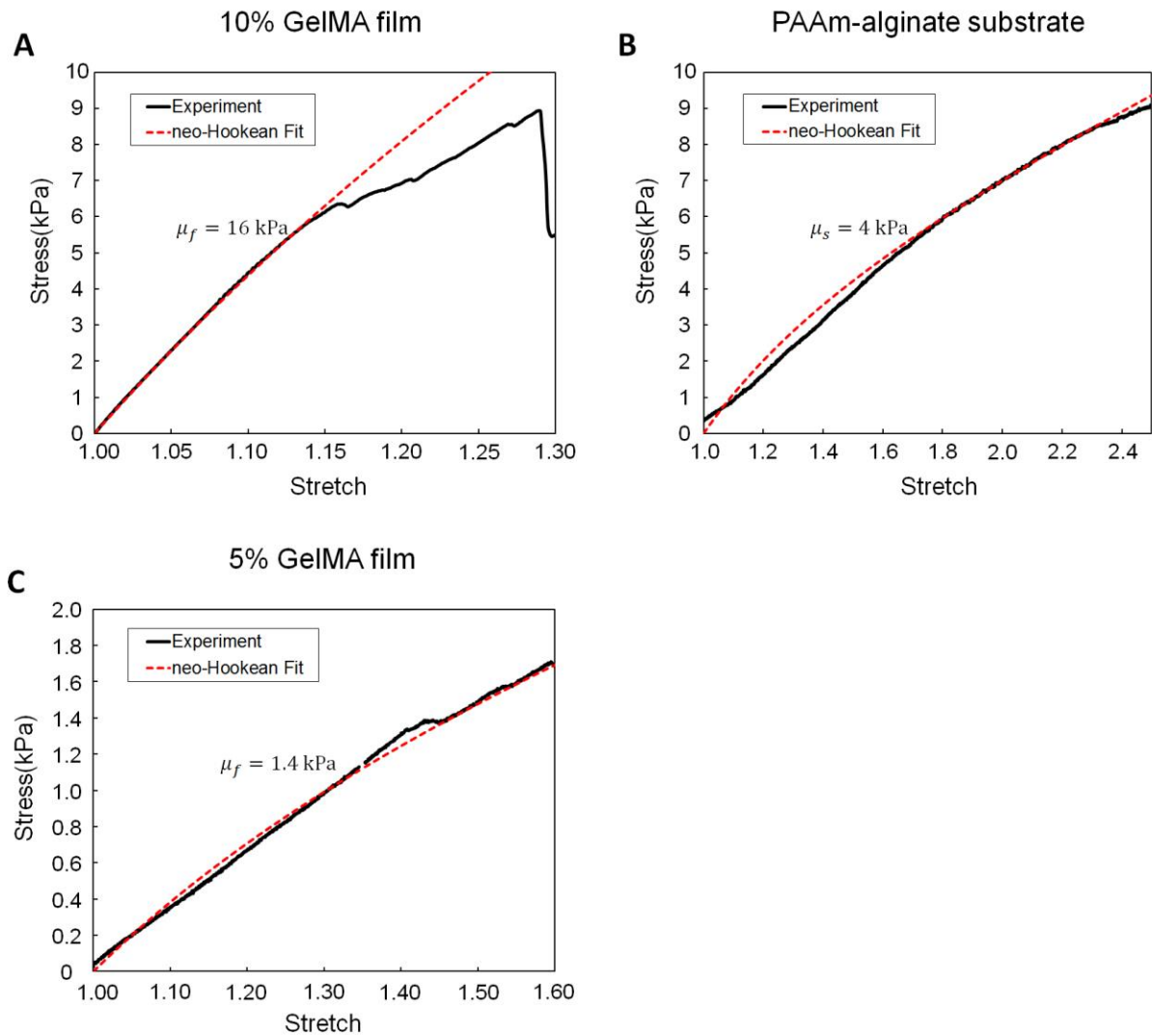
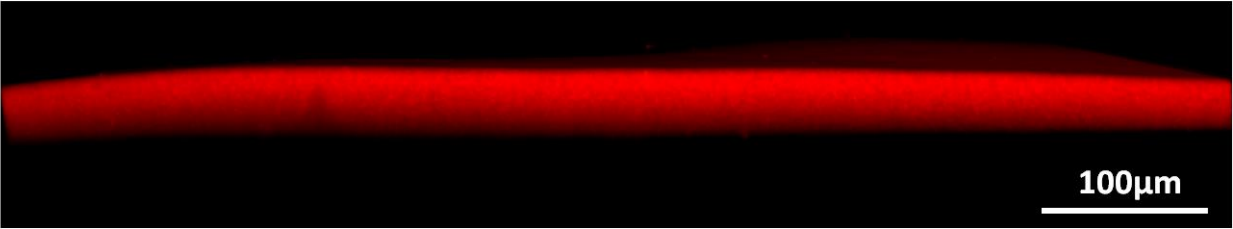


Figure S2. Material characterization and neo-Hookean fit of (A) 10% GelMA film with measured shear moduli 16kPa (B) tough gel substrate with measured shear moduli 4kPa and (C) 5% GelMA film with measured shear moduli 1.4kPa. The resultant film-substrate structure from (A) and (B) has modulus ratio of $\mu_f / \mu_s = 4$, and the resultant film-substrate structure from (C) and (B) has modulus ratio of $\mu_f / \mu_s = 1.4$.

A

$\mu_f / \mu_s = 0.35, \lambda_{ps} = 1.5$ Flat



B

$\mu_f / \mu_s = 0.35, \lambda_{ps} = 2.0$ Crease

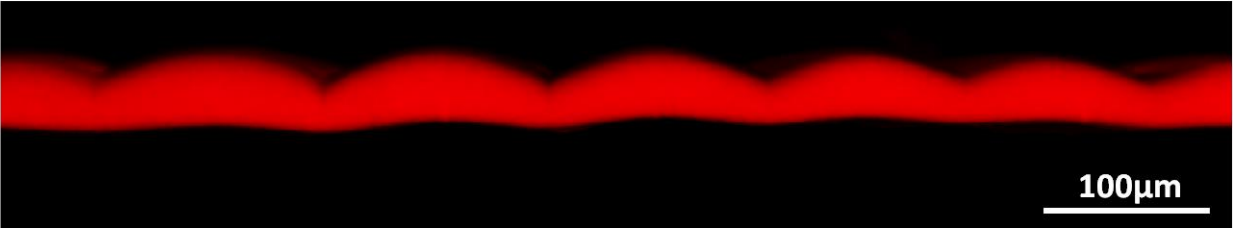


Figure S3. 3D confocal reconstruction of rhodamine b labelled GelMA with film-substrate modulus ratio $\mu_f / \mu_s = 1.4$. When the GelMA film is fully released, (A) the surface remains flat for prescribed substrate pre-stretch of $\lambda_{ps} = 1.5$; (B) crease emerges on the surface for prescribed substrate pre-stretch of $\lambda_{ps} = 2.0$.

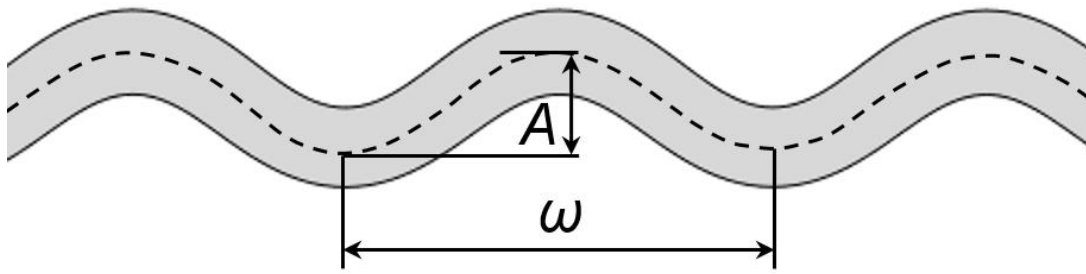


Figure S4. Schematic of the measurement of amplitude A , and wavelength ω of the GelMA morphology. The amplitude A is measured by the peak-valley distance of the neutral axis of the GelMA film. The wavelength ω is measured by the distance between two adjacent peak/valley.

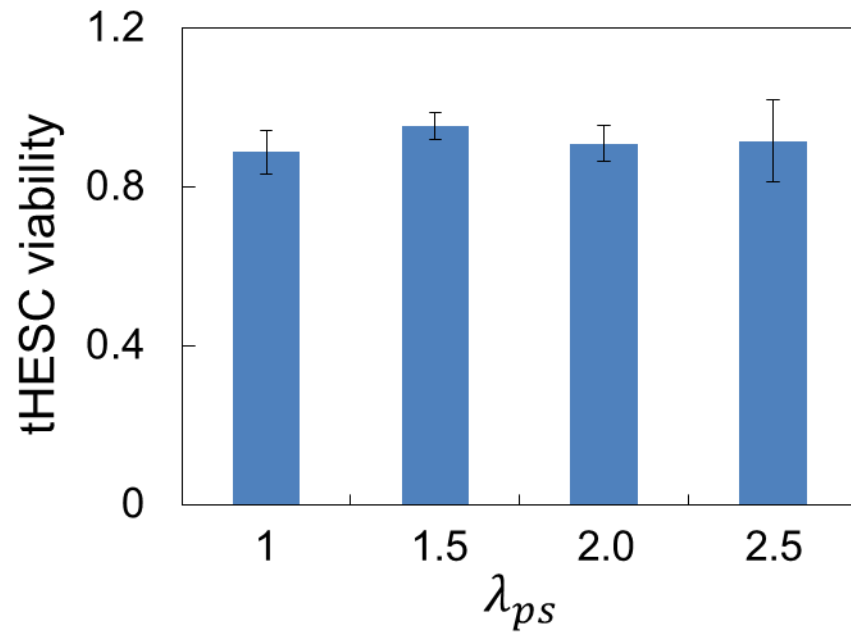


Figure S5. Viability of encapsulated tHESCs in different folded GelMAs prepared at various pre-stretch ratios. Statistical analysis reveals no significant difference in values among all cases ($p > 0.05$).

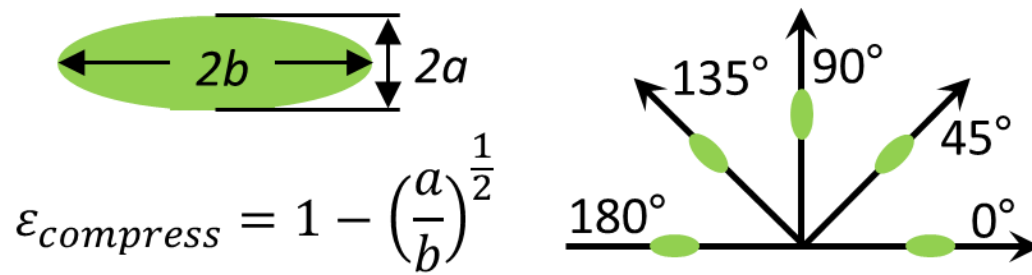


Figure S6. Schematics on calculation of compressive strain and definition of orientation angle for a compressed cell.

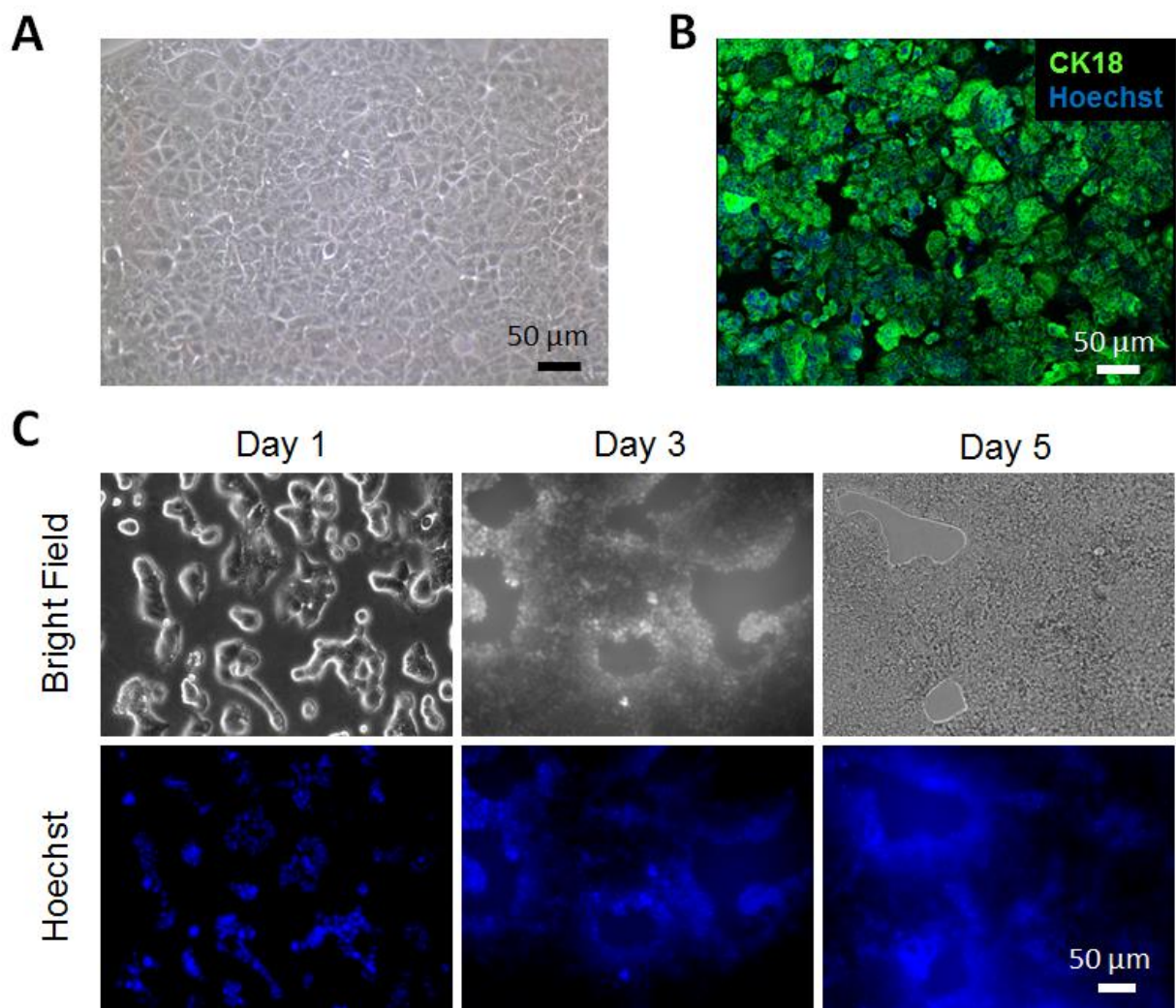


Figure S7. Ishikawa cells cultured in (A) 2D and (B) stained with CK-18 (green) and Hoechst (blue). (C) Images of bright field and cell nuclei of Ishikawa cells (stained with Hoechst) showing cell confluency at day 1, 3 and 5.

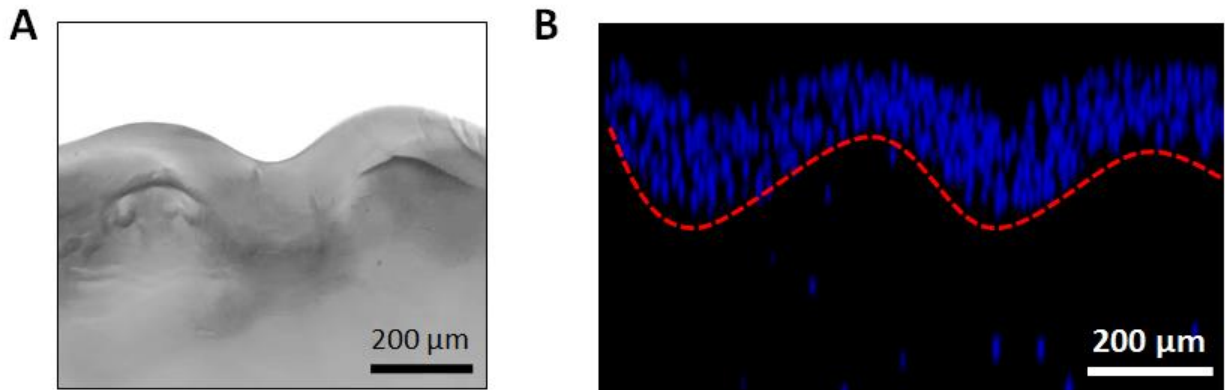


Figure S8. (A) Bright field image showing the boundary between GelMA and tough-hydrogel substrate. (B) 3D reconstruction of z-stack images showing the overlaying of GelMA (encapsulated with blue fluorescent beads at high density) on top of tough-hydrogel substrate (encapsulated with blue fluorescent beads at low density).

Supplementary Table 1. A summary of properties of folded mucosa reported in literature

Location of mucosal folding	Species	Shear modulus (kPa)	Mucosal thickness (μm)	Wavelength (μm)	Morphological pattern	Effective pre-stretch in substrate*	Reference
Bronchus	Pig	~600	~50-300	~600	Folds/Ridges	nr	(3, 4)
Esophagus	Pig	nr	~200-350	~600-1000	Folds/Ridges	nr	(5)
	Mice	nr	~70-200	~200-400	Folds/Ridges	nr	(6)
	Rabbit	nr	~200-400	nr	Folds/Ridges	nr	(7)
	Pig	nr	nr	nr	Folds/Ridges	~1.5	(8)
Large intestine	Rat	~33-3000	~150-200	nr	Ridges	nr	(9-11)
Small intestine	Rat	~1.33-3	nr	nr	Ridges	nr	(12-16)
	Chick	nr	~80-150	~100-200	Ridges	~1.5-2.0	(17)
	Pig	~2	~400-700	nr	Ridges	nr	(18, 19)
Stomach	Human	~0.16	nr	nr	Folds/Ridges	nr	(20)
Urinary bladder	Mouse	nr	nr	nr	Doubles/Ridges	nr	(21)
	Pig	~8	~1000-3000	nr	Doubles/Ridges	nr	(22, 23)
Trachea	Human	nr	nr	nr	Wrinkles/Folds	nr	(24)

nr: not reported.

*: the effective pre-stretch in substrate was evaluated by taking the ratio between the length of the mucosa at the unfolded state (stress-free state) and the length of the substrate with the folded mucosa on it. The mucosa could be separated from the muscle layer, unfolded, and then measured for its length at the unfolded state.

1. Nichol JW, *et al.* (2010) Cell-laden microengineered gelatin methacrylate hydrogels. *Biomaterials* 31(21):5536-5544.
2. Trappmann B, *et al.* (2012) Extracellular-matrix tethering regulates stem-cell fate. *Nature materials* 11(7):642-649.
3. Noble PB, Sharma A, McFawn PK, & Mitchell HW (2005) Elastic properties of the bronchial mucosa: epithelial unfolding and stretch in response to airway inflation. *Journal of applied physiology* 99(6):2061-2066.
4. Wang JY, Mesquida P, & Lee T (2011) Young's modulus measurement on pig trachea and bronchial airways. *Conference proceedings : ... Annual International Conference of the IEEE Engineering in Medicine and Biology Society. IEEE Engineering in Medicine and Biology Society. Annual Conference 2011*:2089-2092.
5. Yang W, Fung TC, Chian KS, & Chong CK (2007) Instability of the two-layered thick-walled esophageal model under the external pressure and circular outer boundary condition. *Journal of biomechanics* 40(3):481-490.

6. Eden K, Rothschild DE, McDaniel DK, Heid B, & Allen IC (2017) Noncanonical NF-kappaB signaling and the essential kinase NIK modulate crucial features associated with eosinophilic esophagitis pathogenesis. *Disease models & mechanisms* 10(12):1517-1527.
7. Lu X & Gregersen H (2001) Regional distribution of axial strain and circumferential residual strain in the layered rabbit oesophagus. *Journal of biomechanics* 34(2):225-233.
8. Zhao J, Chen X, Yang J, Liao D, & Gregersen H (2007) Opening angle and residual strain in a three-layered model of pig oesophagus. *Journal of biomechanics* 40(14):3187-3192.
9. Yang J, Zhao J, Zeng Y, Vinter-Jensen L, & Gregersen H (2003) Morphological properties of zero-stress state in rat large intestine during systemic EGF treatment. *Digestive diseases and sciences* 48(3):442-448.
10. Gao C & Gregersen H (2000) Biomechanical and morphological properties in rat large intestine. *Journal of biomechanics* 33(9):1089-1097.
11. Watters DA, Smith AN, Eastwood MA, Anderson KC, & Elton RA (1985) Mechanical properties of the rat colon: the effect of age, sex and different conditions of storage. *Quarterly journal of experimental physiology* 70(1):151-162.
12. Zhao JB, Sha H, Zhuang FY, & Gregersen H (2002) Morphological properties and residual strain along the small intestine in rats. *World journal of gastroenterology* 8(2):312-317.
13. Dou Y, Fan Y, Zhao J, & Gregersen H (2006) Longitudinal residual strain and stress-strain relationship in rat small intestine. *Biomedical engineering online* 5:37.
14. Sokolis DP (2017) Experimental study and biomechanical characterization for the passive small intestine: Identification of regional differences. *Journal of the mechanical behavior of biomedical materials* 74:93-105.
15. Li J, Zhao J, Liao D, & Gregersen H (2008) Effect of smooth muscle tone on morphometry and residual strain in rat duodenum, jejunum and ileum. *Journal of biomechanics* 41(12):2667-2672.
16. Sun D, Zhao J, Liao D, Chen P, & Gregersen H (2017) Shear Modulus of the Partially Obstructed Rat Small Intestine. *Annals of biomedical engineering* 45(4):1069-1082.
17. Shyer AE, *et al.* (2013) Villification: how the gut gets its villi. *Science* 342(6155):212-218.
18. Gao C, Zhao J, & Gregersen H (2000) Histomorphometry and strain distribution in pig duodenum with reference to zero-stress state. *Digestive diseases and sciences* 45(8):1500-1508.
19. Tan R, *et al.* (2011) Experimental investigation of the small intestine's viscoelasticity for the motion of capsule robot. in *2011 IEEE International Conference on Mechatronics and Automation*.
20. Lim YJ, Deo D, Singh TP, Jones DB, & De S (2009) In situ measurement and modeling of biomechanical response of human cadaveric soft tissues for physics-based surgical simulation. *Surgical endoscopy* 23(6):1298-1307.
21. Chai TC, Russo A, Yu S, & Lu M (2016) Mucosal signaling in the bladder. *Autonomic neuroscience : basic & clinical* 200:49-56.
22. Li C, *et al.* (2014) Quantitative elasticity measurement of urinary bladder wall using laser-induced surface acoustic waves. *Biomedical optics express* 5(12):4313-4328.
23. Dahms SE, Piechota HJ, Dahiya R, Lue TF, & Tanagho EA (1998) Composition and biomechanical properties of the bladder acellular matrix graft: comparative analysis in rat, pig and human. *British journal of urology* 82(3):411-419.
24. Zagalo C, *et al.* (2002) Morphology of trachea in benign human tracheal stenosis: a clinicopathological study of 20 patients undergoing surgery. *Surgical and radiologic anatomy : SRA* 24(3-4):160-168.